

# JAVELIN TRAJECTORY SIMULATION AND ITS USE IN COACHING

MONT HUBBARD

Department of Mechanical Engineering  
University of California  
Davis, CA 95616 USA

Scientific analysis and assessment of athletic performance are, in the general case, notoriously difficult. In track and field events there are at least clearly defined measures of performance (time expired, height jumped, distances thrown, etc.). The coaches' job then becomes one of assisting the athlete to improve his or her technique in order to achieve the optimal performance possible within the constraints imposed by the physical limitations of the athlete. In addition, the coach can suggest exercises and other ways in which these physical limitations (e.g. muscle strength) presently restricting performance can be raised, thus allowing for possible improved performance in the future. In both cases, however, it is the limits of performance which are central.

Shown in Fig. 1 are some distance records for the javelin throw over the past seventy-five years. This history contains several prominent features of interest; a relatively linear increase in distance during the first three decades, a hiatus during World War II followed by a re-establishment of pre-WW II performance at around 70 m, a dramatic increase during the early-to-mid fifties due to the redesign of the javelin into its present aerodynamic shape, and finally a somewhat slower but inexorable increase over the last twenty five years. Examining Fig. 1 one is led to ask what are the limitations on performance. Clearly these limits have not yet been reached.

## COMPARISON OF AERODYNAMICS OF JAVELIN, DISCUS AND SHOT

Of the throwing events (shot, hammer, discus, javelin) the javelin is by far the most aerodynamic. Our intuition that this might be the case is borne out by examining Table 1 in which the shot, discus, and javelin are compared. The first and third rows show that there are large variations in mass and density among the three objects. The large variations in mass result in sizeable variations in achievable initial velocities when thrown by humans (row 4). A more accurate measure of the "aerodynamicity" than the density, however, is the ratio of the maximum possible aerodynamic forces which might act during flight to the (constant) gravity forces.

$$\frac{F_{\text{aero}}}{F_{\text{grav}}} = \frac{\frac{\rho v^2}{2} A C_D}{mg}$$

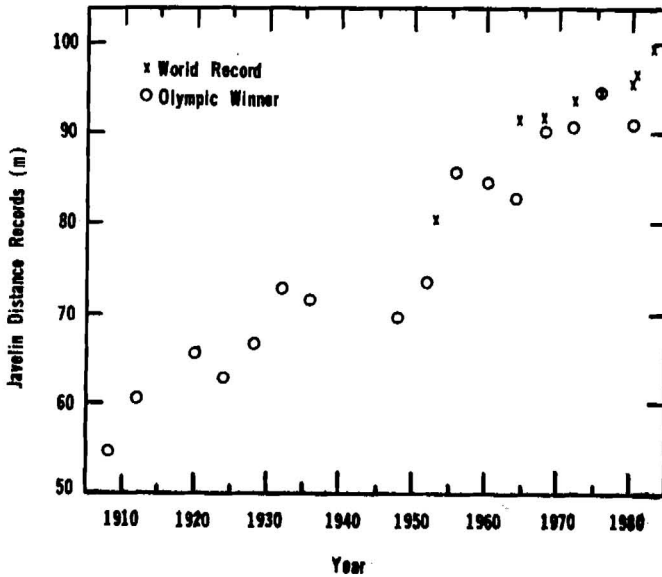


Figure 1. Javelin Olympic distances and world records.

Table 1. Some Physical Characteristics of Shot, Discus and Javelin

	Shot	Discus	Javelin
mass kg	7.2	2.0	0.80
volume $\ell$	0.70	0.90	1.25
density kg/ $\ell$	10.3	2.22	0.64
typical velocity m/sec	15	25	30
maximum vacuum distance m	22	70	95
projected area $m^2$	0.0095	0.039	0.063
inverse mass $kg^{-1}$	0.139	0.50	1.25
drag coefficient	0.47	1.0	1.2
"aerodynamicity" ( $F_{aero}/F_{grav}$ )	0.0072	0.68	4.49

where  $\rho$  = air density,  $v$  = velocity,  $A$  = maximum projected area,  $C_D$  = drag coefficient,  $m$  = object mass, and  $g$  = acceleration of gravity.

Equation (1) can be decomposed in a different way as a product of five factors

$$\frac{F_{\text{aero}}}{F_{\text{grav}}} = \left(\frac{\rho}{2}\right) \left(\frac{v^2}{g}\right) A \left(\frac{1}{m}\right) C_D \quad (2)$$

atmospheric
throw distance
maximum
inverse
shape  
constant
in a vacuum
projected area
mass

which measure, respectively, the contributions of air density, mass specific initial kinetic energy, size, inverse mass, and shape. The last four of these are shown in rows 5-8 of Table 1. In each of these four factors the javelin is greater than the discus and the discus is greater than the shot.

The final row of Table 1 shows that the javelin, according to the measure of Equation (2), is roughly five times as aerodynamic as the discus, which is itself nearly one hundred times as aerodynamic as the shot. The trajectory of the shot may therefore be modeled relatively accurately as a purely ballistic one, while aerodynamic forces must be included in any model for the trajectories of the javelin or discus. Further, for asymmetric shapes like the javelin and discus, aerodynamic forces are a function of not only the magnitude of the relative wind speed but also the attitude of the body relative to the relative wind direction. Thus, initial attitudes and rotations of the body during flight must also be considered.

The general implications of Table 1 are the following. Range of the shot is not appreciably limited by drag; (Soong (1982) has calculated that drag decreases the range by considerably less than 1 percent). While this is not the case for the discus, its asymmetric shape makes it possible to compensate for the decreases in range due to drag by analogous increases in range due to lift generated by appropriate discus attitudes during flight. Indeed, it has also been shown by Soong (1976) that these two factors may nearly cancel, resulting in a range in air nearly equal to that in a vacuum. The even more aerodynamic characteristics of the javelin make it possible for lift to substantially outweigh drag and for the javelin to be thrown roughly 18 percent further in air than in a vacuum (Hubbard, 1984).

#### SIMULATION: RANGE AS A FUNCTION OF INITIAL CONDITIONS

For all the throws, the eventual range depends only (and uniquely) on conditions (position, velocity, attitude, and angular velocity) of the object when released by the thrower. As the "aerodynamicity" increases, however, so does the sensitivity of the eventual range to the above release conditions. Thus, in the case of the javelin especially, it would appear to be of great benefit to focus on the dynamics in flight in order to determine the effects of the initial conditions on range.

Two previous studies of javelin trajectory dynamics (Soong (1975); Red and Zogaib, (1977)) have relied on computer simulation of trajectory equations. These made possible the prediction of dynamic behavior in flight as well as eventual range, entry angle, and time of flight. Unfortunately, the results of these studies were somewhat misleading because: 1) they used theoretical expressions for aerodynamic forces and moments which only poorly approximate the actual forces and moments which act on the javelin in flight, and 2) they did not exhaustively investigate the space of initial conditions in order to determine exactly the set of optimal release conditions.

Recently a similar computer simulation approach has been developed (Hubbard and Rust, 1984a, 1984b; Hubbard, 1984) which incorporates experimentally measured aerodynamic forces and moments from previous javelin wind tunnel tests by Terauds (1972, 1974). From many such simulations it is possible to predict optimum release conditions (initial flight path angle and javelin attitude) as well as sensitivities to perturbations from these optimum conditions and to various environmental conditions (wind, density variations, etc.). In the remainder of the paper we summarize the approach taken in Hubbard and Rust (1984b) and in Hubbard (1984), present for the first time some new vibration free optimal solutions, and discuss how results such as these can be used by throwers and coaches.

In Hubbard and Rust (1984b), the equations of motion for the javelin trajectory are derived from first principles. A particular example trajectory, typical of a good throw, is discussed and the motion of the javelin in flight, obtained by numerically integrating the differential equations, is analyzed. In the companion paper (Hubbard 1984) it was shown, using many such simulations, that when the javelin is thrown in a vertical plane a set of five initial conditions at release determine completely the trajectory and hence the eventual range. This set of initial conditions includes:

1.  $v_0$  - velocity of the center of mass (c.m.)
2.  $z_0$  - height of the c.m.
3.  $\phi_0$  - angle of the velocity vector from horizontal
4.  $\alpha_0$  - angle of attack (angle between the javelin axis of symmetry and the velocity vector)
5.  $\omega_0$  - pitching angular velocity.

These variables are shown in Fig. 2. The subscript 0 above denotes "at time  $t = 0$ ." Although it is always desirable to have  $v_0$  and  $z_0$  as large as possible, there are unique optimal values for the remaining three initial conditions  $\phi_0$ ,  $\alpha_0$ ,  $\omega_0$  which maximize the range. A series of successively less constrained optimum solutions is defined (given  $v_0$  and  $z_0$ ), the last of which is the global optimum javelin trajectory for the remaining three initial conditions.

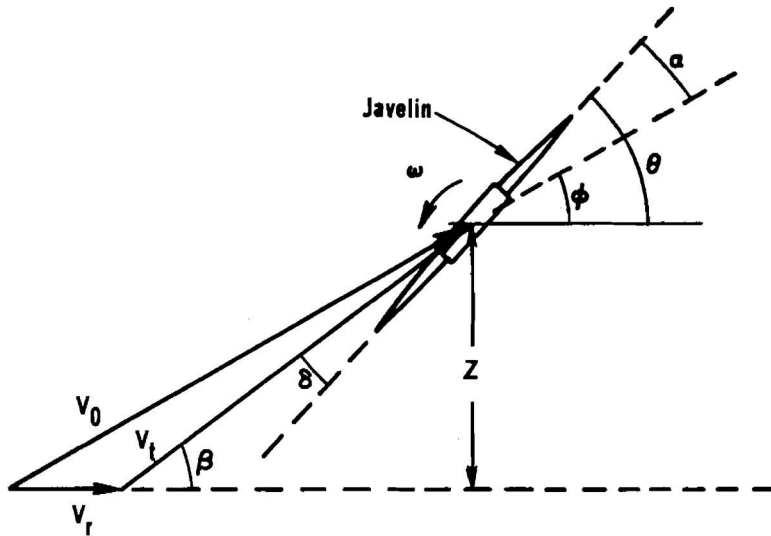


Figure 2. Five initial conditions ( $v_0$ ,  $z_0$ ,  $\phi_0$ ,  $\alpha_0$ ,  $\omega_0$ ) determine subsequent trajectory. Total javelin velocity  $v_0$  is vectorial sum of run-up velocity  $v_r$  and throw velocity  $v_t$ . No transverse vibrations are induced when  $\delta = 0$ .

This optimal solution was found using a three-dimensional Newton-Raphson iterative search. Unfortunately, any attempt to portray or display the behavior of the range in a neighborhood of the optimum is severely limited because of the three-dimensional nature of the space. This may be circumvented, for example, by fixing one of the three variables  $\phi_0$ ,  $\alpha_0$ ,  $\omega_0$  and plotting range contours in the remaining two space.

#### VIBRATION FREE TRAJECTORIES

Another more natural method to decrease the problem dimensionality, however, is to recognize that not all near optimal solutions are equally desirable. Indeed, there is a two-dimensional subspace of the  $\phi_0$ ,  $\alpha_0$ ,  $\omega_0$  three space which is much more preferable from the point of view of minimizing thrower induced vibrations (which can be a severe problem in actual practice). That this is the case may be seen from the following arguments illustrated in Fig. 2.

Because the thrower has a non-zero run-up velocity  $v_r$ , an impulse  $mv_t$  (at an angle  $\beta$  to the horizontal) must be applied to the javelin during the throw in order that a resultant initial velocity  $v_0$  (at angle  $\phi_0$ ) will result. Thus, an impulse of magnitude  $mv_t \sin \delta$  is imparted perpendicular to the javelin axis where the impulse misalignment angle  $\delta$  can be shown (Hubbard, 1984) to be given by

$$\delta = \phi_0 + \alpha_0 - \tan^{-1} \left( \frac{\sin \phi_0}{\cos \phi_0 - v_r/v_0} \right). \quad (3)$$

When  $\delta \neq 0$ , this impulse causes transverse vibrations. If the thrower, however, chooses  $\alpha_0$  to make  $\delta = 0$ , i.e. throws at an initial angle of attack

$$\alpha_0 = \tan^{-1} \left( \frac{\sin \phi_0}{\cos \phi_0 - v_r/v_0} \right) - \phi_0 \quad (4)$$

then the subsequent trajectory will be vibration free. Figure 3 shows the dependence of the vibration free initial angle of attack on  $\phi_0$ . We emphasize that, although the initial angle of attack  $\alpha_0$  is non-zero, there would be no thrower induced vibrations in this case since all the throwing impulse is imparted along the javelin axis (or "through the point").

Having thus reduced the dimensionality of the initial condition space to two by choosing  $\alpha_0$  according to (4), we may then present contours of constant range in the  $\phi_0, \omega_0$  two space. Shown in Fig. 4 are such contours of constant range for the Held-90 javelin assuming that  $\alpha_0$  satisfies (4) and that  $z_0 = 2\text{m}$ ,  $v_r = 6 \text{ m/s}$ , and  $v_0 = 30.48 - 0.127(\phi_0 - 35) \text{ m/s}$ . This variation of initial velocity  $v_0$  with flight path

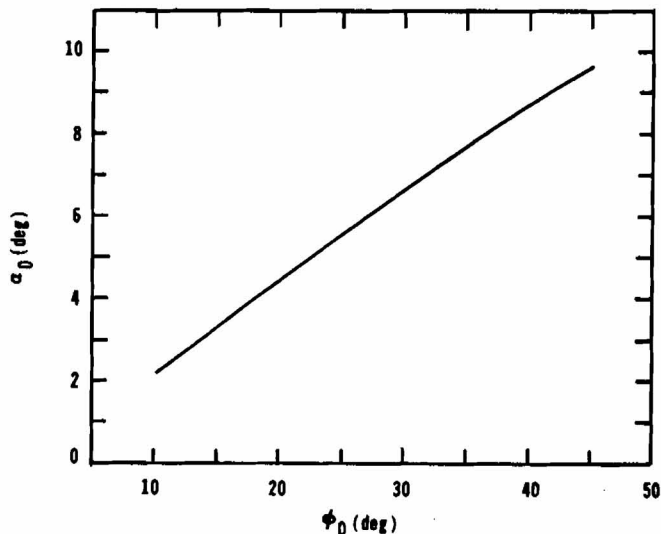


Figure 3. Initial angle of attack which minimizes thrower induced vibrations.

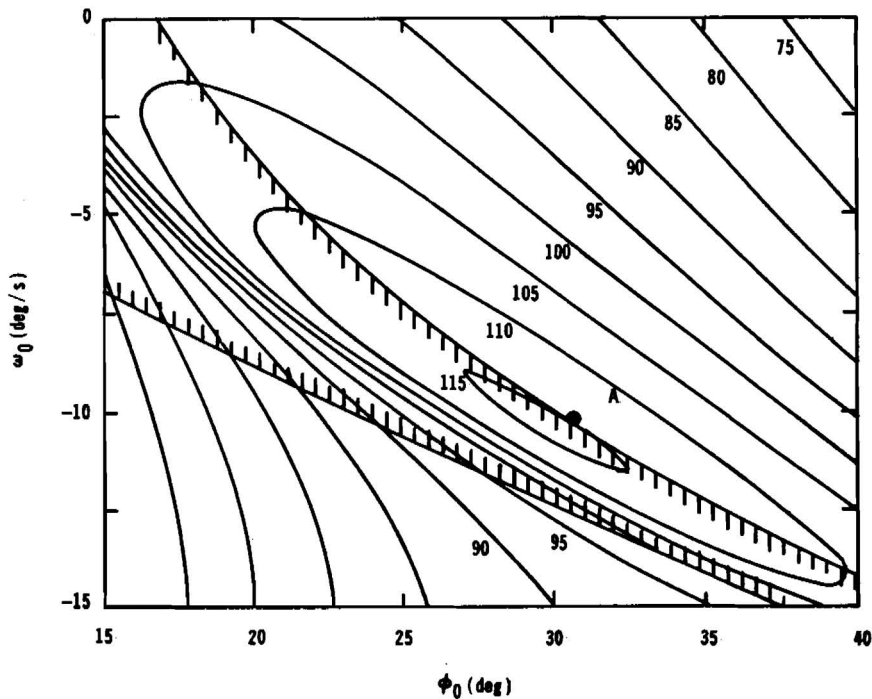


Figure 4. Vibrationless range contours for Held-90 javelin vs  $\phi_0$  and  $\omega_0$  (contour interval = 5 m). Hashed region corresponds to tail first landings.

angle  $\phi_0$  is an attempt, first suggested by Red and Zogaib (1977), to model their experimentally observed fact that it is possible to throw faster at smaller initial flight path angles,  $\phi_0$ . Also shown in Fig. 4 are two contours of zero entry angle, between which (in the hashed region) the javelin strikes the ground tail first, thus resulting in an illegal (unmeasurable) throw. Thus, the optimal deterministic initial conditions  $\phi_0^*$ ,  $\omega_0^*$  are those which maximize the range outside this region (i.e. subject to the entry angle constraint,  $\theta_f < 0$ ). From Fig. 4, these optimal initial conditions can be seen to be very near the point  $(\phi_0^*, \omega_0^*) = (31 \text{ deg}, -10.4 \text{ deg/s})$  and to result in a range of approximately 114.8 m. The optimal point is denoted by  $\bullet$  in Fig. 4.

Fig. 5 shows, in the same  $\phi_0$ ,  $\omega_0$  space, contours of constant time of flight,  $t_f$ . As is clear from the figure, the time of flight can vary rather dramatically in the range  $1.98 < t_f < 5.73$  sec, the optimum time of flight ( $t_f^* = 5.26$  sec) occurring at the optimal values of  $\phi_0^*$  and  $\omega_0^*$  above which maximize the range.

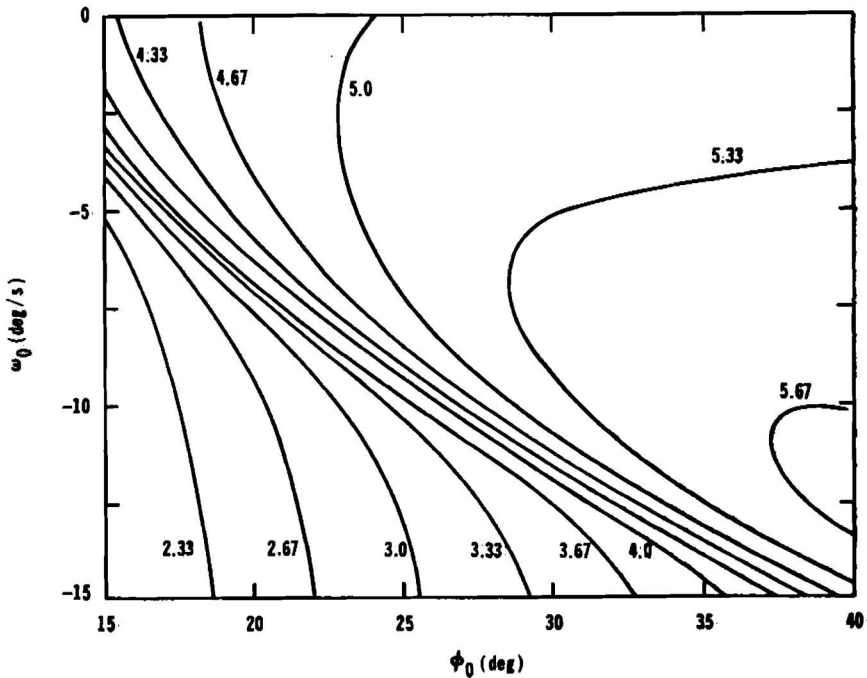


Figure 5. Time of flight contours (in seconds) for vibration free throw.

#### PROBABILISTIC INTERPRETATION OF INITIAL CONDITIONS

Probably the main additional information conveyed by Fig. 4 (beyond the set of theoretically optimal initial conditions  $\phi_0^*$ ,  $\alpha_0^*$ ,  $\omega_0^*$ ) is the extremely sensitive nature of the solution. The angular velocities  $\omega_0$  in question are very small (being roughly of the order of magnitude of the second hand on a clock, 6 deg/sec). It is therefore unlikely that  $\omega_0$  may be controlled by the thrower with much precision.

Indeed, a more realistic description of the "choice" of the initial conditions by the thrower may be a statistical or probabilistic one. That is, the thrower may be able to choose mean values  $\bar{\phi}$ ,  $\bar{\omega}$  for the variables  $\phi_0$ ,  $\omega_0$ , with the actual values being randomly determined, perhaps normally distributed about these means, with variances  $\sigma_\phi^2$  and  $\sigma_\omega^2$  which are inversely proportional to the degree of control which the thrower has over each variable. For example, assuming that  $\alpha_0$  is determined by (4) above, and assuming statistical independence of  $\phi_0$  and  $\omega_0$ , the joint probability density function of the particular initial condition  $\phi_0$ ,  $\omega_0$  might be approximated as jointly Gaussian,



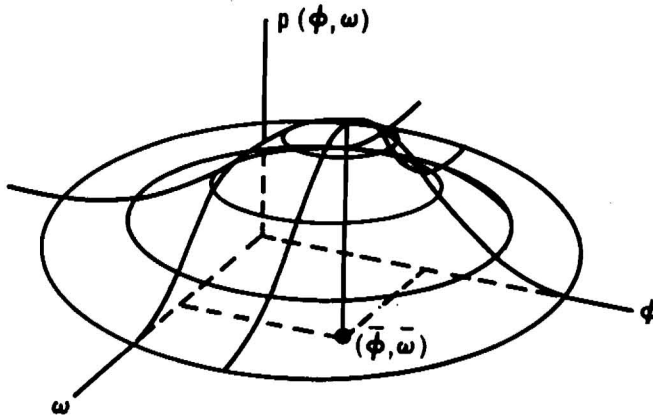


Figure 6. Joint Gaussian probability density function for  $\phi_0$ ,  $\omega_0$  when considered as random variables. The most probable value for  $\phi_0$ ,  $\omega_0$  is the mean  $\bar{\phi}$ ,  $\bar{\omega}$ .

$$p(\phi_0, \omega_0) = \frac{1}{2\pi\sigma_\phi\sigma_\omega} \exp \left[ -\frac{(\phi_0 - \bar{\phi})^2}{2\sigma_\phi^2} - \frac{(\omega_0 - \bar{\omega})^2}{2\sigma_\omega^2} \right] \quad (5)$$

where  $\bar{\phi}$ ,  $\bar{\omega}$  are the mean values and  $\sigma_\phi$ ,  $\sigma_\omega$  are the standard deviations of  $\phi_0$  and  $\omega_0$ . Figure 6 shows the nature of the  $p(\phi_0, \omega_0)$  surface. Reasonable estimates can be made for  $\sigma_\phi$ . Based on experimental data (Miller and Munro, 1983), it appears that  $\sigma_\phi$  is roughly of the order of 1-2 deg. Estimation of  $\sigma_\omega$  is more problematic, however, since it is extremely difficult to measure such small angular velocities accurately. No reports in the open literature are known which contain such measurements and on which estimates of  $\sigma_\omega$  might be based.

#### CHOICE OF THE OPTIMAL AIM POINT $\bar{\phi}^*$ , $\bar{\omega}^*$

In any case, such inexact control of initial conditions turns the problem for the thrower into one of stochastic optimization. Namely, he or she must choose  $\bar{\phi}$ ,  $\bar{\omega}$  (which might be termed an "aim point") to maximize some payoff function of the range. One possibility for such a performance index would be the expected value of the range. Thus, the thrower might choose  $\bar{\phi}^*$ ,  $\bar{\omega}^*$  which maximizes the expected range

$$\iint p(\phi_0, \omega_0) R(\phi_0, \omega_0) e(\phi_0, \omega_0) d\phi_0 d\omega_0 \quad (6)$$

where  $p(\phi_0, \omega_0)$  is given by (5),  $R(\phi_0, \omega_0)$  is the range function whose contours are shown in Fig. 4 and which must be evaluated by simulation, and  $e(\phi_0, \omega_0)$  is either one or zero depending on whether the final entry angle constraint is satisfied or not. Thus, in this scheme illegal throws are not weighted at all.

The point here is that, when inexact control exists, it is probably better to aim not for the deterministic optimum which lies on the zero entry angle contour (point ● in Fig. 4) but instead for a point somewhat away from the deterministic optimum (point A in Fig. 4). This is because, due to uncontrollable stochastic variations in the initial conditions, the former alternative will lead to roughly one half of all throws being illegal because they strike tail first. Obviously, the above ideas generalize to the three degree-of-freedom case where the thrower is free to choose all three initial conditions,  $\phi_0, \alpha_0, \omega_0$ .

#### INTERPRETATION AND USE OF RESULTS

Although most of the initial sections have been concerned with the description of a specific model and optimization procedure, one of the main purposes of this paper is to discuss how these results can be used by coaches and participants. The most obvious use of the information in Fig. 4 is for the calculation of a best aim point  $\bar{\phi}^*, \bar{\omega}^*$  as discussed above.

The mathematical maximization of (6) by choosing the best aim point  $\bar{\phi}^*, \bar{\omega}^*$  is a rather formidable set of calculations, however. Instead, it should probably be possible simply to use the sensitivity information conveyed in the contour spacing in Fig. 4 to make a reasonable guess for the location of the best aim point without making the lengthy calculations. The thrower would then attempt to match (or nearly match) his or her mean initial conditions in a throw to the aim point.

The use of the aim point concept will be most useful when there is the provision for more or less immediate feedback to the thrower regarding performance. High speed video tape and/or inertial instrumentation of the javelin, perhaps even in concert, are two possible ways to achieve this feedback, which is essential if the thrower is to be able to modify performance iteratively and home in on the best aim point. The feasibility of such techniques is presently being studied.

Repeated solution of the problem (namely, generation of Fig. 4) for different nominal velocities  $v_{nom}$  in  $v_0 = v_{nom} + 0.127(\phi - 35)$  can answer questions concerning how the optimal initial conditions might change as a thrower's velocity capability increases. Such a study is included in Hubbard (1984) and is a specific example of the calculation of the sensitivity of the limits of performance to thrower physical limitations mentioned in the opening paragraph above.

Finally, the results and approaches outlined herein may be used in the study and design of new javelins. As throwers' capabilities increase, gradual modifications in javelin design will be necessary. Using simulation, it may be possible to determine the optimum shape of the pitching

moment profile, which is apparently the main aerodynamic change which results when the javelin shape is perturbed slightly.

## CONCLUSIONS

Numerical simulation of the differential equations describing javelin flight has been discussed. Many such simulations can map the initial condition space into range and can be used as a basis for determination of the optimal way to throw a javelin with given aerodynamic characteristics. Vibration free trajectories can be assured by choosing the initial angle of attack so that the impulse misalignment angle is made zero. Deterministic range contours in the initial condition space may be used for the computation of best aim points if reliable and accurate estimates can be made of the stochastic variability of the thrower for each initial condition. Feedback to the throwers of their performance will be necessary for them to be able to converge to aim points. Computer simulation also appears to hold promise in the design process for javelins of the future.

## REFERENCES

- Miller, D. I. and C. F. Munro (1983) "Javelin Position and Velocity Patterns During Final Foot Plant Preceding Release," Journal of Human Movement Studies, 9, 1-20.
- Red, W. E., and A. J. Zogaib (1977) "Javelin Dynamics Including Body Interaction," J. appl. Mech., 44(3), 496-498.
- Soong, T.-C. (1975) "The Dynamics of Javelin Throw," J. appl. Mech., 42(2), 257-262.
- Soong, T.-C. (1976) "The Dynamics of Discus Throw," J. appl. Mech., 43(4), 531-536.
- Soong, T.-C. (1982) "Biomechanical Analyses and Applications of Shot Put and Discus and Javelin Throws," in Human Body Dynamics; Impact, Occupational and Athletic Aspects, D. N. Ghista (ed.), Clarendon Press, Oxford.
- Terauds, J. (1972) "A Comparative Analysis of the Aerodynamics and Ballistic Characteristics of Competition Javelins," Ph.D. Dissertation, University of Maryland, College Park.
- Terauds, J. (1974) "Wind Tunnel Tests of Competition Javelins," Track and Field Quarterly Review, 74(2), 88-95.